Available online at www.sciencedirect.com
SCIENCE DIRECT®
Diamond and Related Materials 12 (2003) 422–428
DIAMOND AND RELATED MATERIALS
www.elsevier.com/locate/diamond

# Electrical and field emission investigation of individual carbon nanotubes from plasma enhanced chemical vapour deposition

W.I. Milne[a,*], K.B.K. Teo[a], M. Chhowalla[a], G.A.J. Amaratunga[a], S.B. Lee[b], D.G. Hasko[b], H. Ahmed[b], O. Groening[c], P. Legagneux[d], L. Gangloff[d], J.P. Schnell[d], G. Pirio[d], D. Pribat[d], M. Castignolles[e], A. Loiseau[e], V. Semet[f], Vu Thien Binh[f]

[a]*Department of Engineering, University of Cambridge, Trumpington Street, Cambridge CB2 1PZ, UK*
[b]*Microelectronics Research Centre, Cavendish Laboratory, University of Cambridge, Cambridge, UK*
[c]*University of Fribourg, Fribourg, Switzerland*
[d]*Thales Research and Technology, Orsay, France*
[e]*University of Montpellier and CNRS-ONERA, Montpellier, France*
[f]*University of Lyon, Lyon, France*

**Abstract**

Plasma enhanced chemical vapour deposition (PECVD) is a controlled technique for the production of vertically aligned multiwall carbon nanotubes for field emission applications. In this paper, we investigate the electrical properties of individual carbon nanotubes which is important for designing field emission devices. PECVD nanotubes exhibit a room temperature resistance of 1–10 k$\Omega/\mu$m length (resistivity $10^{-6}$ to $10^{-5}$ $\Omega$ m) and have a maximum current carrying capability of 0.2–2 mA (current density $10^7$–$10^8$ A/cm$^2$). The field emission characteristics show that the field enhancement of the structures is strongly related to the geometry (height/radius) of the structures and maximum emission currents of $\sim$10 $\mu$A were obtained. The failure of nanotubes under field emission is also discussed.
© 2002 Elsevier Science B.V. All rights reserved.

*Keywords:* Nanotubes; Electrical characterisation; Field emission; Plasma chemical vapour deposition

## 1. Introduction

Carbon nanotubes are an unique form of carbon filament/fiber in which the graphene layers roll up to form tubes [1]. There are several properties of carbon nanotubes which make them extraordinary materials for field emission. Firstly, with graphene layers parallel to the filament axis, nanotubes (single wall metallic-type or multiwall) exhibit high electrical conductivity at room temperature. Secondly, nanotubes are high in aspect ratio and whisker-like in shape. Utsumi [2] evaluated commonly used field emission tip shapes and concluded that the best field emission tip should be whisker-like (i.e. nanotube), followed by the sharpened pyramid, hemispheroidal, and pyramidal shapes which are typically seen in metal or silicon tips. Thirdly, nanotubes can be very stable emitters, even at high temperatures. Purcell et al. [3] demonstrated that a multiwall nanotube emitter could be heated up by its emission current up to 2000 K and remain stable, unlike metal emitters which suffer from thermal runaway. For a multiwall nanotube, its resistance decreases with temperature which limits ohmic heat generation, and surface diffusion is less likely in the strong C–C covalent bonds of the carbon nanotube. These unique characteristics of carbon nanotubes make them remarkable field emitters.

Carbon nanotubes have already been applied in various field emission applications such as displays [4], lamps [5], arc arrestors [6] and X-ray sources [7]. Among these, we are interested in three applications, namely displays, parallel electron beam lithography, and microwave amplifiers, as shown schematically in Fig. 1. In most applications today, nanotubes are first mass-produced by arc discharge as this is presently the most cost-effective production technique [8]. The arc discharge nanotubes are purified and mixed with an epoxy/

*Corresponding author. Tel.: +44-1223-332757; fax: +44-1223-766207.
*E-mail address:* wim@eng.cam.ac.uk (W.I. Milne).

0925-9635/03/$ - see front matter © 2002 Elsevier Science B.V. All rights reserved.
PII: S0925-9635(02)00292-3

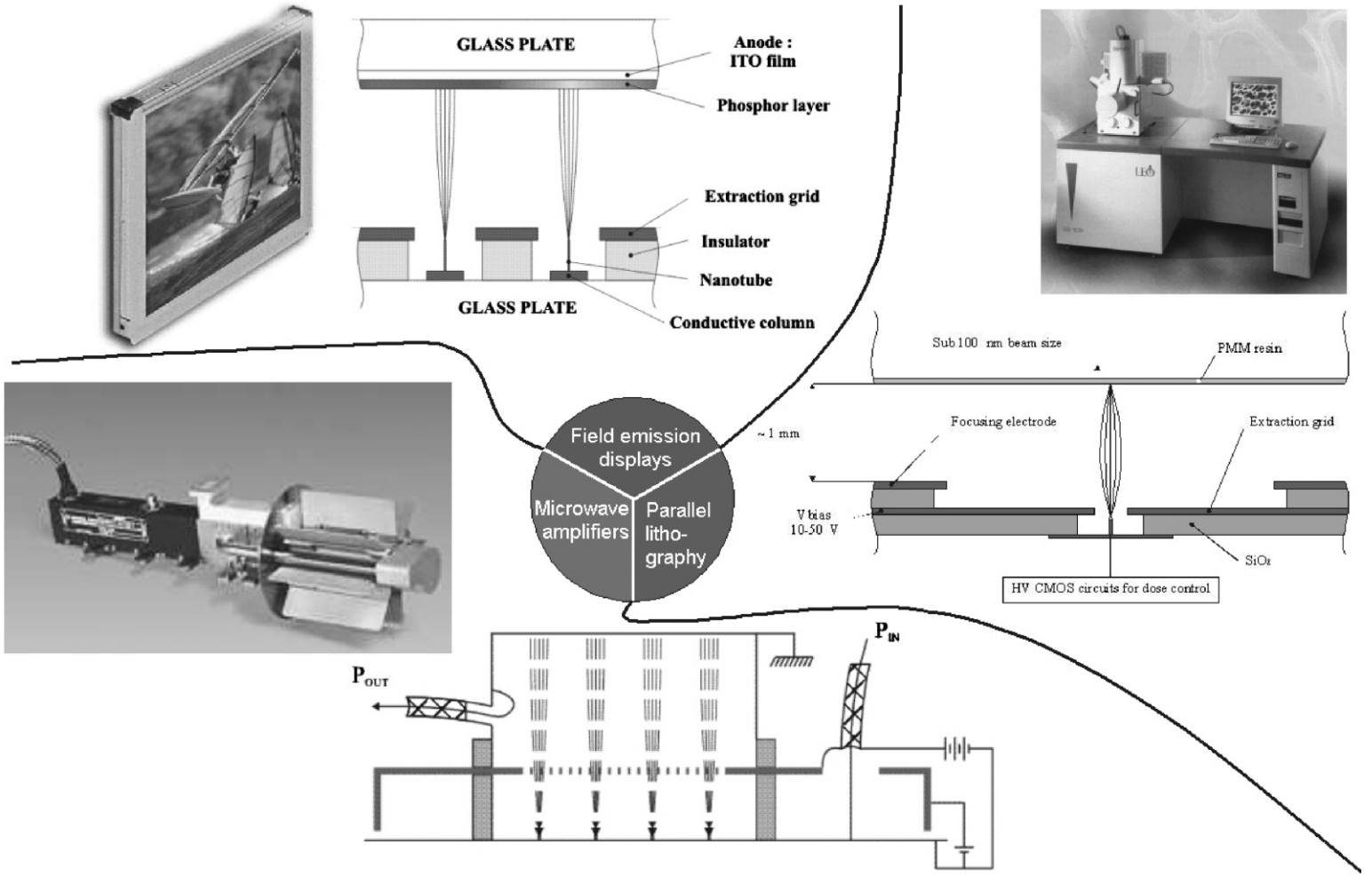


Fig. 1. Various applications using carbon nanotube emitters which we are currently investigating.

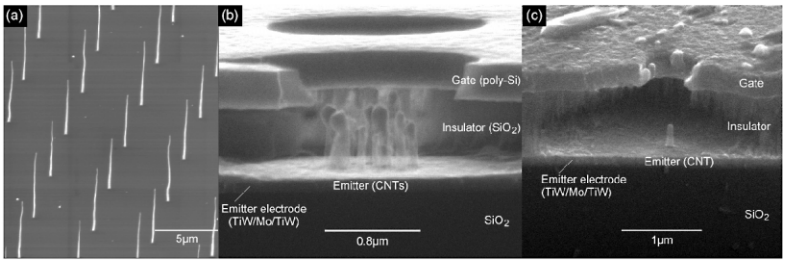


Fig. 2. Various examples of PECVD carbon nanotube emitters: (a) in the form of an array of tips; (b) in a multiple nanotube microcathode [13]; and (c) in a single nanotube microcathode.

binder, and then screen printed or applied at emitter locations, such as that used in Ref. [9]. Alternatively, electrophoresis could be used to adhere the arc discharge nanotubes in solution to specific electrodes [10]. Practically speaking, these strategies are useful only for 'macroscopic' field emission sources, because the carbon nanotubes are 'randomly' distributed and mostly unoriented.

The motivation behind this work is the controlled production of micro-field emission sources based on carbon nanotubes. Such electron sources could be used as the microguns for parallel electron beam lithography [11], but would also equally be applicable in 'macroscopic' applications such as field emission displays and microwave amplifiers. We have chosen to pursue the production of nanotubes via the plasma enhanced chemical vapour deposition (PECVD) technique, which was first pioneered by Ren et al. [12]. Using this method, it is possible to achieve highly controlled growth (in terms of height, diameter, placement and alignment) of multiwalled carbon nanotubes and produce operational field emission microcathodes [13] as shown in Fig. 2. These examples show that PECVD is indeed a feasible solution for carbon nanotube deposition for technological purposes.

Having demonstrated the feasibility of the process to successfully produce emission sources, it is now timely to take one step back and measure the fundamental properties, such as resistivity, maximum current density, field emission characteristics, enhancement factor, of individual nanotubes from the PECVD process. These fundamental data would be invaluable for the design of future devices based on individual nanotubes and are thus the focus of the experimental work presented in this paper.

## 2. Experimental details

The carbon nanotubes were produced using a d.c.-PECVD system which is described in detail elsewhere [14]. Briefly, the substrates are prepared by sputtering a Ni catalyst thin film onto a diffusion barrier layer on Si substrates. The diffusion barrier layer is used to prevent Ni diffusion/reaction with the Si at high temperatures to form $NiSi_x$ which impedes the formation of nanotubes [15]. Typical diffusion barriers are insulating $SiO_2$ or conductive TiN, and only a thin film (10–20 nm) of this material is necessary to prevent the diffusion/reaction of Ni with the Si substrate. The substrates were then transferred to a PECVD chamber which was evacuated to $10^{-2}$ Torr by a rotary pump. The substrates were heated to 700 °C at which the Ni thin film formed nanoclusters due to surface tension effects [14]. These nanoclusters seeded the growth of the carbon nanotubes which was performed by PECVD of acetylene ($C_2H_2$) and ammonia ($NH_3$) for 15 min. The $C_2H_2$ provides the carbon for nanotube growth, whereas the $NH_3$ etches the amorphous carbon (a-C) by-products from the process to give truly a-C free deposition which is suitable for electron device fabrication [16]. Transmission electron microscopy of the PECVD nanotubes reveal that they are bamboo in structure, with 20–40 graphene layers running parallel to the nanotube axis as shown in Fig. 3.

The electrical characteristics of individual nanotubes were determined by fabricating suspended nanotube bridges and measuring their $I$–$V$ characteristics [17]. The field emission characteristics of individual nanotubes were investigated using a scanning anode field emission system on a vertical array such as that shown in Fig. 2a. The spacing used in the array was 25 μm which allowed us to probe the characteristics of individ-

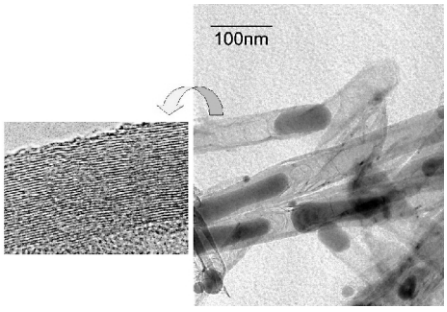


Fig. 3. Transmission electron micrograph of PECVD nanotubes.

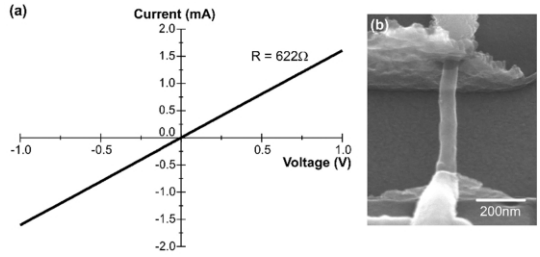


Fig. 4. (a) The low voltage *I–V* characteristic of a suspended PECVD carbon nanotube; and (b) the SEM of the nanotube under test.

ual emitters. Although the emission characteristics of individual nanotube/fiber emitters have been previously performed by other groups [18,19], the methodology presented here is distinctively different because there is no need to know absolute distance between the anode and the sample in order to measure the enhancement factor of the structures.

## 3. Results and discussion

### *3.1. Electrical conductivity measurements*

Conductivity measurements were performed on ten suspended nanotubes, such as that shown in Fig. 4. All nanotubes exhibited *I–V* characteristics that were ohmic/linear at low positive and negative applied voltages. A typical room temperature *I–V* of a 55-nm diameter, 600-nm long section of nanotube is shown in Fig. 4. The linearity of this *I–V* curve indicates that there is no contact barrier between the metal electrodes used (Nb in this case) and the carbon nanotube. Note that as this is a two contact measurement, the resistance measured is the sum total of the contact resistance and the nanotube resistance, and hence the resistances measured here are slightly higher than the actual resistance of the nanotube.

The resistance of the section of nanotube in Fig. 4 was 622 Ω, which corresponds to 1.04 kΩ/μm of nanotube length. None of the ten nanotubes measured showed a gating effect when an electric field was applied using a third electrode, indicating that the nanotubes were conductive (i.e. non-semiconducting) in nature. The room temperature resistances of the nanotubes were mostly in the range of 1–10 kΩ/μm length. If conduction was assumed to be through the entire cylindrical cross sectional area of the nanotube, the resistivity of the nanotube in Fig. 4 is $2\times10^{-6}$ Ω m. Indeed, the range of resistivities observed over several suspended nanotube bridges were between $10^{-6}$ and $10^{-5}$ Ω m. These values compare very well to arc discharge multiwall nanotubes in the literature [20], where the resistivity is calculated to be $9\times10^{-6}$ Ω m for a 350-nm long section of a 20-nm diameter nanotube whose resistance was 10 kΩ. In general, the resistivities of multiwall nanotubes compare well with arc-grown graphite fibers and ropes of single wall nanotubes whose resistivities are $\sim10^{-6}$ Ω m [21,22].

Temperature dependent resistance measurements were also performed on a couple of PECVD nanotubes. These showed a small increase in resistance as the temperature was lowered from 300 to 4.2 K as presented in Ref. [17]. The increase in resistance at lower temperatures indicates that the nanotubes have thermally activated defects (activation energy extracted was 30 meV) which do contribute to the conduction at room temperature (since $kT=26$ meV) [23]. It is interesting that arc discharge multiwall nanotubes [20] also exhibit a similar increase in resistance at lower temperatures. However, this behaviour is opposite to that of well crystallised arc grown graphite fibers or single crystal graphite whose resistances decrease at lower temperatures, characteristic of 'metallic' behaviour where electron–phonon scattering is reduced at lower temperatures [21].

The nanotube of Fig. 4 was electrically stressed by increasing the voltage until breakdown occurred at 2 mA. This corresponded to a maximum current density of $8.4\times10^{7}$ A/cm$^2$ if one were to assume that conduction occurred through the entire cross sectional area of the nanotube. All the nanotubes tested exhibited initial breakdown at currents between 0.2 and 2 mA, which corresponds to current densities of $10^{7}$–$10^{8}$ A/cm$^2$. This is one to two orders of magnitude higher than the maximum current density ($\sim10^{6}$ A/cm$^2$ [24]) that a metal wire would typically carry before electromigration induced breakdown occurs, demonstrating that these PECVD grown nanotubes are capable of carrying very high current densities indeed.

### *3.2. Field emission measurements*

The following procedure was employed to determine the field enhancement factor (β) of the nanotube emitters in an array from scanning anode field emission measurements. A current conditioning process (in the micro-ampere range) was applied to drive off the adsorbates on the emitter tips to yield reproducible Fowler–Nordheim type emission, as is discussed in our previous work [25]. The scanning anode used in these experiments was tip/conical shaped with a 1-μm radius and a 90° cone angle, and further information on the system used can be found in Ref. [26].

The position of each emitter was determined by performing a constant voltage scan (i.e. current maxima indicates emitter positions) or a constant current scan (i.e. voltage minima indicates emitter positions). The anode was then situated directly above a particular emitter and an *I–V* ramp was performed, as shown in Fig. 5. The Fowler–Nordheim parameters were then extracted assuming a work function of 4.9 eV [27] for

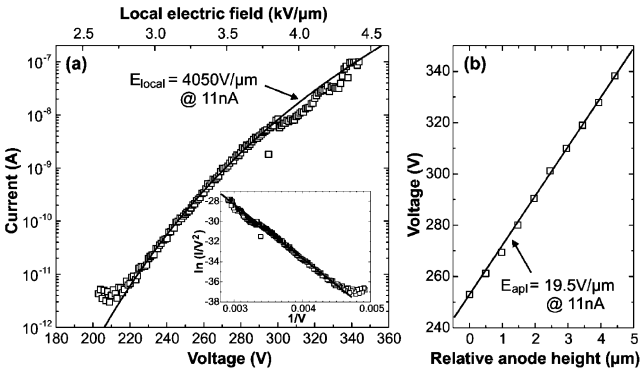


Fig. 5. (a) $I$–$V$ and $I$–$E_{\text{local}}$ characteristics for a typical nanotube emitter. The solid curve is the FN fit derived from the FN plot in the inset. (b) $\Delta V/\Delta z$ measurement to obtain $E_{\text{apl}}$ for a fixed current of 11 nA.

the nanotube emitter, and the measurement curve was re-expressed in terms of $I$–$E_{\text{local}}$. The scale for $E_{\text{local}}$ is expressed in the top scale bar of Fig. 5.

As $E_{\text{local}} = E_{\text{apl}}\beta$ it was necessary to measure the applied electric field ($E_{\text{apl}}$) at a particular current in order to obtain the field enhancement factor ($\beta$). The method employed here is similar to that used by Karabutov et al. [28] and Andrienko et al. [29] who used a scanning probe to investigate electron emission from CVD diamond films. First, a fixed current of 11 nA was extracted from the emitter using voltage $V_1$. Then, the anode was then raised vertically by a short distance ($\Delta z$), and a new voltage $V_2$ was determined in order to extract the same emission current of 11 nA; the voltage difference $\Delta V$ being $V_2 - V_1$. The electric field applied by the anode ($E_{\text{apl}}$) to extract 11 nA was then calculated as $\Delta V/\Delta z$.

To physically understand this measurement of $E_{\text{apl}}$, a simulation was performed using FlexPDE v2.22 to derive the voltage distribution between a nanotube and the tip-shape anode placed 10 μm above it (later, it will be shown that the actual height was ~10 μm, and so this simulation is valid). As can be seen in the potential distribution of Fig. 6a, there is a region of 'flat' potential lines from the middle of the gap to just above the nanotube. The voltage in this region has a linear dependence with distance (Fig. 6b), which indicates that this is a region of constant field. Assuming the nanotube is directly beneath the apex of the anode (i.e. within 1.5 μm in radius), the radial field variation in this constant field region is 2% from the simulation. Thus, essentially a uniform field, i.e. $E_{\text{apl}}$, is being applied to the nanotube from the anode directly above it.

By moving the anode upwards by a short distance $\Delta z$ and applying $\Delta V$ more voltage to maintain the same emission current, this constant field region is simply being extended in distance. This is because the same field must be present there in order to induce the same local field at the emitter to extract the same emission current. Thus, the measurement of $\Delta V/\Delta z$ is a measure of the field in the constant field region, which is equivalent to $E_{\text{apl}}$. This was quantitatively verified by a second simulation at 11 μm height (i.e. $\Delta z = 1$ μm) where a voltage $\Delta V = E_{\text{apl}}$ more was required to maintain the same field in the constant field region and at the nanotube apex.

Returning now to the actual measurement, Fig. 5b plots the voltage against relative anode height for the nanotube under investigation, and indeed a linear slope ($E_{\text{apl}} = \Delta V/\Delta z = 19.5$ V/μm) was found. From the $I$–$V$ and $I$–$E_{\text{local}}$ characteristic of Fig. 5a, the applied voltage and local field ($E_{\text{local}}$) to extract 11 nA was 312 V and 4050 V/μm, respectively. Thus, $\beta = E_{\text{local}}/E_{\text{apl}} = 208$.

Incidentally, the 'approximate' height of the anode could be obtained by extrapolating the $\Delta V/\Delta z$ characteristic of Fig. 5b to give the $x$-intercept (i.e. distance to '0 V potential'). This gave the approximate anode height to be ~13 μm. Note that this is an overestimation of the height because the linear ($\Delta V/\Delta z$) region has a relatively shallow slope between the anode and emitter (Fig. 6b). It is not desirable to obtain the anode height by crashing it into the sample because this could potentially damage the anode (e.g. change the tip-shape) or the sample itself (e.g. landing on a nanotube).

Altogether, the $\beta$ of ten emitters were determined using the above method. These ten emitters were then observed by SEM and their heights ($h$) and radii ($r$) were measured. The average height of the nanotubes was 5.83 μm and average radius was 24 nm. The field enhancement factor, for a rounded-whisker conductive emitter in a uniform field, is given by the approximation $h/r$ for $h \gg r$ [2]. The $\beta$ from SEM measurements ($\beta_{\text{SEM}}$) were compared with $\beta$ from field emission measurements ($\beta_{\text{FE}}$) in Fig. 7. It is evident that $\beta_{\text{FE}}$ and $\beta_{\text{SEM}}$ for seven out of the ten emitters are in good agreement with each other (within the ±12% lines). Moreover, the average $\beta_{\text{SEM}}$ of 249 corresponded well to the average $\beta_{\text{FE}}$ of 242. This good agreement here confirms that the emission mechanism from these nan-

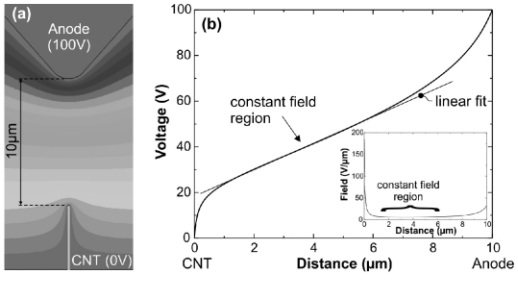


Fig. 6. Simulation of the anode 10 μm above a nanotube (CNT). The potential distribution is given in (a) with each band denoting 5 V potential change. The voltage distribution in the gap is given in (b) with the corresponding field distribution in the inset.

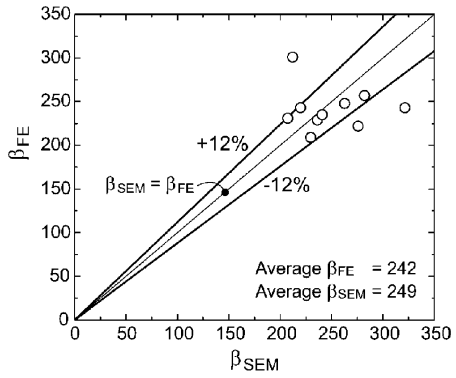


Fig. 7. (a) $I$–$E_{apl}$ characteristics of a typical nanotube. The maximum currents reached were 10–20 μA before failure. (b) Simulated up-rooting electrostatic force on a 5-μm tall, 50-nm diameter nanotube using the measurement geometry of (a).

otubes was conventional geometrically enhanced field electron emission.

Finally, the maximum emission currents extracted from individual nanotubes were between 10 and 20 μA at applied electric fields ($E_{apl}$) of ~25 V/μm, above which failure would occur with an abrupt drop in emission current. Fig. 8a shows an $I$–$E$ characteristic of a typical nanotube emitter from 0.1 pA to 10 μA in emission current. The maximum currents reached during emission was significantly lower than the maximum currents (~1 mA) carried by a single nanotube during direct contact d.c. measurements in the conductivity measurements. Post examination of the sample after emission measurements revealed that nanotubes which have failed during emission stress measurements were missing or left a crater. This suggested that the nanotubes could be up-rooted due to electrostatic forces. The simulation geometry of Fig. 5a was then used to calculate the electrostatic force on a 5-μm tall, 50-nm diameter nanotube under various $E_{apl}$ from the anode as shown in Fig. 8b. At $E_{apl}$=25 V/μm, the simulation yielded an upward electrostatic force of 0.76 μN on the nanotube, which is equal to 390 MPa of tensile stress

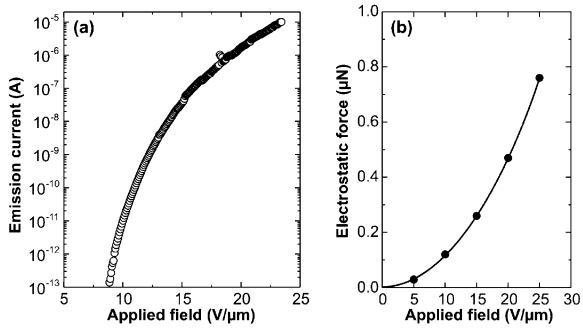


Fig. 8. $\beta_{FE}$ from emission measurements compared with $\beta_{SEM}$ which was calculated from the height/radius ratio, determined by SEM.

at the interface between the nanotube and the diffusion barrier/substrate at failure. In comparable terms, this is equivalent to 31 kg of weight pulling on a 1-mm diameter joint between two materials, which represents a substantial loading on the joint indeed! This significant tensile stress probably caused the failure at the nanotube: substrate interface.

## 4. Conclusions

We have presented electrical and field emission measurements of individual carbon nanotubes produced by the PECVD process. Electrical conductivity measurements on individual carbon nanotubes reveal that they exhibit a room temperature resistance of 1–10 kΩ/μm length (resistivity $10^{-6}$ to $10^{-5}$ Ω m) and have a maximum current carrying capability of 0.2–2 mA (current density $10^7$–$10^8$ A/cm$^2$). All the PECVD nanotubes examined were conductive in nature. From our field emission measurements, it was found that the field enhancement from individual nanotubes was due to the aspect ratio of their whisker-like structure. This means that it is possible to tailor the geometry (diameter controlled by catalyst size, height controlled by deposition time) of the nanotube to obtain a desirable β for certain applications. Individual nanotubes could emit currents of ~10 μA. It is proposed that the nanotubes failed at these currents due to the large electrostatic force exerted by the anode. Having characterised the electrical properties of the nanotubes produced by PECVD, it is now possible to design suitable emitter structures for various applications.

## References

[1] S. Ijima, Nature 354 (1991) 56.
[2] T. Utsumi, IEEE Trans. Electron. Dev. 38 (1991) 2276.
[3] S.T. Purcell, P. Vincent, C. Journet, V. Thien Binh, Phys. Rev. Lett. 88 (2002) 105502.
[4] D.S. Chung, S.H. Park, H.W. Lee, et al., Appl. Phys. Lett. 80 (2002) 4045.
[5] J.-M. Bonard, T. Stockli, O. Noury, A. Chatelain, Appl. Phys. Lett. 78 (2001) 2775.
[6] R. Rosen, W. Simendinger, C. Debbault, et al., Appl. Phys. Lett. 76 (2000) 1197.
[7] G.Z. Yue, Q. Qiu, B. Gao, et al., Appl. Phys. Lett. 81 (2001) 355.
[8] Presentation at Materials Week 2001 by Matthieu Grac of Nanoledge, France.
[9] W.B. Choi, D.S. Chung, J.H. Kang, et al., Appl. Phys. Lett. 75 (1999) 3129.
[10] W.B. Choi, Y.W. Jin, H.Y. Kim, et al., Appl. Phys. Lett. 78 (2001) 1547.
[11] P. Legagneux, G. Pirio, E. Balossier, et al., A revisited concept for parallel e-beam lithography, Phantoms Newsletter, 5, 2002.
[12] Z.F. Ren, Z.P. Huang, J.W. Xu, et al., Science 282 (1998) 1105.
[13] G. Pirio, P. Legagneux, D. Pribat, et al., Nanotechnology 13 (2002) 1.
[14] M. Chhowalla, K.B.K. Teo, C. Ducati, et al., J. Appl. Phys. 90 (2001) 5308.

[15] K.B.K. Teo, M. Chhowalla, G.A.J. Amaratunga, et al., Mat. Res. Soc. Symp. Proc. 675 (2001) W9.1.
[16] K.B.K. Teo, M. Chhowalla, G.A.J. Amaratunga, et al., J. Vac. Sci. Tech. B 20 (2002) 116.
[17] S.B. Lee, K.B.K. Teo, M. Chhowalla, et al., Microelectron. Eng. 61–62 (2002) 475.
[18] L.R. Baylor, V.I. Merkulov, E.D. Ellis, et al., J. Appl. Phys. 91 (2002) 4602.
[19] J.-M. Bonard, K.A. Dean, B.F. Coll, C. Klinke, Phys. Rev. Lett. 89 (2002) 197602.
[20] C. Schonenberger, A. Bachtold, C. Strunk, J.-P. Salvetat, L. Forro, Appl. Phys. A 69 (1999) 283.
[21] L. Forro, C. Schnonenberger, in: M.S. Dresselhaus, G. Dresselhaus, Ph. Avouris (Eds.), Carbon Nanotubes, Springer, 2001, pp. 329–391.
[22] A. Thess, R. Lee, P. Nikolaev, et al., Science 273 (1996) 483.
[23] T.W. Ebbesen, H.J. Lezec, H. Hiura, J.W. Bennett, H.F. Ghaemi, T. Thio, Nature 382 (1996) 54.
[24] CRC Handbook of Chemistry and Physics, sixty third ed., Chemical Rubber Corp., Boca Raton, FL, 1983.
[25] V. Semet, V. Thien Binh, P. Vincent, et al., Appl. Phys. Lett. 81 (2002) 343.
[26] L. Nilsson, O. Groening, O. Kuettel, P. Groening, L. Schlapbach, J. Vac. Sci. Tech. B 20 (2002) 326.
[27] O. Groening, O.M. Kuttel, P. Groening, Ch. Emmeneggar, P. Groening, L. Schlapbach, J. Vac. Sci. Tech. B 18 (2000) 665.
[28] A.V. Karabutov, V.D. Frolov, S.M. Pimenov, V.I. Konov, Diamond Relat. Mater. 8 (1999) 763.
[29] I. Andrienko, A. Cimmino, D. Hoxley, S. Prawer, R. Kalish, Appl. Phys. Lett. 77 (2000) 1221.